Title	Predissociation of oxygen in the B 3Σ-u state
Author(s)	Chiu, SSL; Cheung, ASC; Finch, M; Jamieson, MJ; Yoshino, K; Dalgarno, A; Parkinson, WH
Citation	The Journal Of Chemical Physics, 1992, v. 97 n. 3, p. 1787-1792
Issued Date	1992
URL	http://hdl.handle.net/10722/147713
Rights	Creative Commons: Attribution 3.0 Hong Kong License

Predissociation of oxygen in the $B\,^3\Sigma_u^-$ state

S. S-L. Chiu[a] and A. S-C. Cheung[b]
Department of Chemistry, University of Hong Kong, Hong Kong

M. Finch,[c] M. J. Jamieson,[d] K. Yoshino, A. Dalgarno, and W. H. Parkinson
Harvard-Smithsonian Center for Astrophysics, Cambridge, Massachusetts 02138

(Received 3 December 1991; accepted 22 April 1992)

The predissociation linewidths and level shifts of vibrational levels of three oxygen isotopic molecules $^{16}O_2$, $^{16}O^{18}O$, and $^{18}O_2$ arising from the interactions of the $B\,^3\Sigma_u^-$ state with the four repulsive states $^5\Pi_u$, $^3\Sigma_u^+$, $^3\Pi_u$, and $^1\Pi_u$, have been calculated. A set of parameters characterizing these interactions has been determined. Good agreement between calculated and experimental predissociation widths and shifts has been obtained for all the three isotopic molecules.

I. INTRODUCTION

The predissociation of the oxygen molecule in the Schumann–Runge bands ($B\,^3\Sigma_u^- - X\,^3\Sigma_g^-$) has been studied extensively, both experimentally and theoretically.[1–21] The effect of predissociation on spectral features can be detected by measurements of linewidth and level shifts. Accurate spectroscopic constants and linewidths published for various vibrational levels of the three oxygen isotopic molecules, $^{16}O_2$, $^{16}O^{18}O$, and $^{18}O_2$,[17–20,22,23] have been determined in recent experiments.

It has been shown[6,7] that the predissociation is dominated by the interaction with the $^5\Pi_u$ state with lesser roles being played by the $^3\Sigma_u^+$, $^3\Pi_u$, and $^1\Pi_u$ states. Figure 1 shows the four repulsive states crossing the $B\,^3\Sigma_u^-$ state.[24]

In this paper, we derive a single set of parameters, characterizing the interaction potentials, that fits simultaneously the predissociation linewidths and the second vibrational differences of the energy levels of the $B\,^3\Sigma_u^-$ states of the three isotopic molecules.

II. METHOD OF CALCULATION AND RESULTS

A. Method of calculation

The rotation–vibration levels of the $B\,^3\Sigma_u^-$ state are dissociated through spin–orbit coupling to the $^1\Pi_u$, $^5\Pi_u$, and $2\,^3\Sigma_u^+$ repulsive states and through spin–orbit and electronic–rotational coupling to the $^3\Pi_u$ repulsive state. In an analysis of early linewidth data, Schaefer and Miller[2] had concluded that electronic–rotational coupling is much weaker than spin–orbit coupling and Yang *et al.*[21] have argued from a study of rotationally resolved spectra that the electronic–rotational coupling matrix element is two orders of magnitude smaller than the spin–orbit coupling matrix element. We have used the hypothesis of pure precession in an explicit evaluation of the matrix element and we confirm that electronic–rotational coupling is negligible at the low rotational levels $J < 10$ with which this paper is concerned.

The unperturbed $B\,^3\Sigma_u^-$ potential curve is well established. In our calculations we used a Rydberg–Klein–Rees potential constructed from the observations of Cheung *et al.*[22] We adopted the Born–Oppenheimer approximation so that the same potentials and couplings apply for each of the isotopes $^{16}O_2$, $^{16}O^{18}O$, and $^{18}O_2$. The spin–orbit couplings between the $B\,^3\Sigma_u^-$ state and the repulsive states were assumed to be independent of internuclear distance.

We used the exponential form of the repulsive state potentials suggested by Julienne and Krauss[6] as did Cheung *et al.*[17]

$$V(R) = V_x \exp[-(M_x/V_x)(R-R_x)], \tag{1}$$

where R denotes the internuclear distance, V_x and M_x are the energies and slopes at the crossing points, R_x, and the potential energy is measured from the $O(^3P) + O(^3P)$ energy of infinite separation. For each of the four repulsive states we determined the parameters R_x and M_x and the coupling strength, A_x, to the $B\,^3\Sigma_u^-$ state. The predissociation width and level shift contribution are calculated for the F_2 component of the Schumann–Runge band and are independent of the Hund's coupling case. The calculated spin–orbit coupling matrix element for the $B\,^3\Sigma_u^- - ^5\Pi_u$ interaction has to be multiplied by an angular factor $(7/6)^{1/2}$ in the determination of the width and shift (see Table II of Julienne and Krauss[6]). The direct couplings of the repulsive states are negligible. Measurements have been made of the widths[18,19] and shifts[17,22,23] of many rotational–vibrational levels of the upper $B\,^3\Sigma_u^-$ state for all three isotopes. We adjusted the twelve parameters (R_x, M_x, and A_x for each repulsive state) to make our theoretical predictions of the widths and shifts match as closely as possible the measured values. We searched the twelve-dimensional space to get the best least-squares fit using the calculated parameters of Julienne and Krauss[6] ($R_x = 1.875$ Å, $M_x = 40\,000$ cm^{-1} Å^{-1}, $A_x = 65$ cm^{-1}) as starting values for the dominant $^5\Pi_u$ state. For this research, we took the rotational quantum number N to be 0.

[a] Present address: Department of Chemistry, University of Manchester, Manchester M13 9PL, United Kingdom.
[b] International Exchange Scholar, Smithsonian Institution, 1990–1992.
[c] Present address: Department of Physics, Georgia Institute of Technology, Atlanta, Georgia.
[d] Permanent address: Department of Computing Science, University of Glasgow, Glasgow G12 8QQ, Scotland.

 0021-9606/92/151787-06$006.00

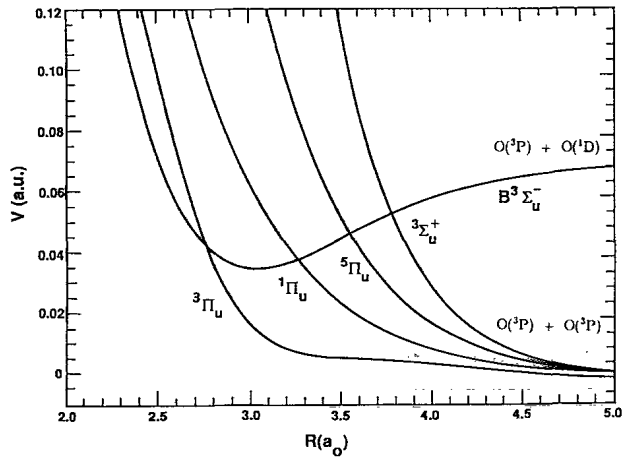

FIG. 1. Some potential energy curves of O_2. The curves are labeled by the molecular state designations.

Because all the couplings are small, we used a sequence of two-state approximations to determine the theoretical widths and shifts for each repulsive state and for each set of trial parameters and we assumed the effects to be additive. For the widths it was necessary to average over the three fine-structure components F_i to produce the total widths; the weighting factors are given by Julienne and Krauss.[6] The calculations of the shifts and widths were carried out by the method of Du *et al.*[25] In it, the bound vibrational levels of the $B\,^3\Sigma_u^-$ state and the Green's function for the Hamiltonian of the relevant repulsive state are determined numerically. The Green's function is obtained from the regular and irregular solutions of the Schrödinger equation for the repulsive state and the shift is given as a double quadrature. The relevant second order differential equations were solved by the Numerov method, the secant method was employed to find the energy levels in the $B\,^3\Sigma_u^-$ potential and the quadratures were done by Simpson's rule.

An initial search in the R_x, M_x, and A_x space was made in a comparison of the widths alone between theory and experiment. The best least-squares fit was made for the $^5\Pi_u$ state only, since it is the dominant one for most of the vibrational levels. The other repulsive states were then introduced iteratively, all the parameters being adjusted by means of a trial and error search on the tabulated values to get the best least-squares fit. Of the three parameters the sensitivity to R_x was greatest and a finer grid was used in the R_x subspace than in the subspaces of M_x and A_x. A good set of value of the parameters was found which is shown in Table I(a). The search was then extended to include the shifts. We attempted to find the smoothest fit for the deperturbed second vibrational energy level differences, obtained by adding the calculated energy shifts to the measured energies. The deperturbation technique is described in detail by Julienne and Krauss,[6] by Cheung *et al.*,[17] and by Lefebvre-Brion and Field.[26] A least-squares fit was made to fit the deperturbed second differences for each isotopic molecule as a cubic polynomial function of the vibrational quantum number. The quality of the fits was measured by the statistical function $100\% \times \Sigma_i (y_i^f - \bar{y})^2/\Sigma_i (y_i - \bar{y})^2$, where the sums are over the measurements y_i, y_i^f are the fitted values and $\bar{y}$ is the mean. The search in the parameter space was made to maximize the statistical function. A slightly different set of values of the parameters was found which is shown in Table I(b). With the values of Table I(a), 54% of the shifts fall within the experimental data spread and those outside missed by an average of 0.14 cm^{-1}. The parameters in Table I(b) are better for the shifts with 64% of them in the experimental spread and an average miss of 0.12 cm^{-1}. The parameters listed in Table I(a) yielded the best compromise between a good fit to the widths and a smooth deperturbation of the shifts. At the present state of measurement and theoretical calculation we recommend the values reported in Table I(a).

B. Linewidths

The published studies on the linewidths of the Schumann–Runge bands have been discussed in detail by Cheung *et al.*[18] and Chiu *et al.*[19] for $^{16}O^{18}O$ and $^{18}O_2$. The linewidths presented in those papers are believed to be the most accurate currently available because they are independent of instrumental width and obtained from direct fitting of measured absorption cross sections with the best available molecular constants[17,22,23] in calculating the line center positions of the fine structure components. These linewidths, Γ_{exp}, were used to optimize the model parameters in this study.

Tables II–IV show, for $^{16}O_2$, $^{16}O^{18}O$, $^{18}O_2$, the calculated partial width due to each repulsive state, the total F_2 width $\Gamma(F_2)$ and the average width $\bar{\Gamma}$ of the three F_i components with the same J (but different N). This average width is independent of J for each of the interactions and is equal to 20/21, 2/3, 4/3, and 2/3 of the F_2 width for interaction with the respective $^5\Pi_u$, $^3\Sigma_u^+$, $^3\Pi_u$, and $^1\Pi_u$

TABLE I. Alternative sets of open channel parameters for the interactions with the $B\,^3\Sigma_u^-$ state.

	(a)[a]				(b)[b]			
State	$^5\Pi_u$	$^3\Sigma_u^+$	$^3\Pi_u$	$^1\Pi_u$	$^5\Pi_u$	$^3\Sigma_u^+$	$^3\Pi_u$	$^1\Pi_u$
A_x (cm^{-1})	70	46	35	33	67	33	41	35
R_x (Å)	1.879	1.999	1.429	1.711	1.879	1.999	1.436	1.712
M_x (cm^{-1} $Å^{-1}$)	38 600	49 000	74 000	25 000	38 600	49 000	74 000	25 000

[a]The parameters in (a) give a superior fit to the widths.
[b]The parameters in (b) give a superior fit to the shifts (see text).

TABLE II. Calculated partial and total FWHM predissociation widths (cm^{-1}) of the $B\,^3\Sigma_u^-$ state of $^{16}O_2$.

v	$^5\Pi_u$	$^3\Sigma_u^+$	$^3\Pi_u$	$^1\Pi_u$	$\Gamma(F_2)$	$\bar{\Gamma}$	Γ_{exp}[a]
0	0.000	0.000	0.012	0.289	0.301	0.209	
1	0.002	0.000	0.050	1.222	1.274	0.884	0.93
2	0.080	0.000	0.117	0.000	0.197	0.232	0.72
3	0.932	0.000	0.201	0.533	1.667	1.511	1.78
4	3.202	0.008	0.285	0.436	3.930	3.725	3.87
5	1.569	0.100	0.351	0.067	2.087	2.073	2.13
6	0.724	0.549	0.388	0.018	1.678	1.584	1.79
7	0.874	0.944	0.393	0.152	2.362	2.086	2.01
8	1.182	0.101	0.371	0.256	1.910	1.858	1.92
9	0.005	0.433	0.331	0.274	1.043	0.917	1.01
10	0.611	0.036	0.281	0.232	1.159	1.135	1.09
11	0.900	0.360	0.228	0.170	1.658	1.515	1.48
12	0.394	0.099	0.178	0.113	0.785	0.755	0.88

[a]Values from Cheung *et al.* (Ref. 18).

TABLE IV. Calculated partial and total FWHM predissociation widths (cm^{-1}) of the $B\,^3\Sigma_u^-$ state of $^{18}O_2$.

v	$^5\Pi_u$	$^3\Sigma_u^+$	$^3\Pi_u$	$^1\Pi_u$	$\Gamma(F_2)$	$\bar{\Gamma}$	Γ_{exp}[a]
0	0.000	0.000	0.010	0.260	0.270	0.187	
1	0.001	0.000	0.043	1.249	1.292	0.890	
2	0.044	0.000	0.103	0.023	0.171	0.195	
3	0.608	0.000	0.185	0.638	1.431	1.251	1.53
4	2.765	0.003	0.271	0.338	3.376	3.222	3.23
5	2.630	0.044	0.344	0.007	3.025	2.998	3.12
6	0.082	0.328	0.391	0.106	0.907	0.889	1.05
7	1.756	0.927	0.407	0.287	3.376	3.023	2.77
8	0.382	0.523	0.394	0.332	1.630	1.458	1.32
9	0.468	0.103	0.358	0.264	1.193	1.168	1.18
10	1.161	0.397	0.316	0.164	2.030	1.892	1.71
11	0.355	0.172	0.256	0.081	0.865	0.849	0.84
12	0.013	0.064	0.204	0.031	0.312	0.348	

[a]Values from Chiu *et al.* (Ref. 19).

states.[6,7] Plots of the predissociation linewidths vs vibrational quantum number v from Tables II–IV are presented in Fig. 2 for $^{16}O_2$, $^{16}O^{18}O$, and $^{18}O_2$. In order to illustrate that the oscillatory structure is shared by the different isotopic species, the widths are plotted against a mass-reduced scale, $\rho(v+\frac{1}{2})$, where ρ is the square root of the ratio of the reduced masses of the isotope and $^{16}O_2$. The dashed curve is a curve that passes through the theoretical widths of all three isotopes. The points are the experimental data of Cheung *et al.* (Ref. 18) and Chiu *et al.* (Ref. 19).

From Tables II–IV, it is evident that the $^5\Pi_u$ interaction is the most important overall and it gives rise to the basic features of the width pattern with maximum widths at $v=4$ for all three isotopes and subsidiary maxima at $v=7$ and 11 for $^{16}O_2$, and $v=7$ and 10 for $^{16}O^{18}O$ and $^{18}O_2$. The $^3\Sigma_u^+$ state contributes significantly to the total width from $v=6$ to 12, and it contributes nearly the same amount as the $^5\Pi_u$ state to the total width at $v=7$ for all isotopes. The contributions of the $^3\Pi_u$ and $^1\Pi_u$ states are quite similar, $\sim$0.1–0.4 cm^{-1} from $v=5$ to 12. The $^1\Pi_u$ state has a significantly larger contribution to the total width at $v=1$ for all the isotopes. Since the experimental linewidth is available only from $^{16}O_2$ at $v=1$, the parameters determined for the $^1\Pi_u$ state are not of high accuracy. The contribution of the $^3\Pi_u$ state to the total width is not large but is significant. Wodtke *et al.*[16] suggested that the $^3\Pi_u$ gives the dominant contribution to the $v=11$ level of $^{16}O_2$, in their dispersed laser-induced fluorescence spectra, but their conclusion is not supported in this study.

The partial width from the $^5\Pi_u$ interaction is nearly zero at $v=9$ of $^{16}O_2$, which implies that the assumption of using equal widths for the components in the least-squares fit to obtain experimental linewidths from absolute absorption cross sections is not appropriate.[6] In fact, Cheung *et al.*[18] reported having difficulty in fitting the (9,0) band of $^{16}O_2$ earlier. Further work to improve the fitting of the

TABLE III. Calculated partial and total FWHM predissociation widths (cm^{-1}) of the $B\,^3\Sigma_u^-$ state of $^{16}O^{18}O$.

v	$^5\Pi_u$	$^3\Sigma_u^+$	$^3\Pi_u$	$^1\Pi_u$	$\Gamma(F_2)$	$\bar{\Gamma}$	Γ_{exp}[a]
0	0.000	0.000	0.011	0.275	0.286	0.198	
1	0.002	0.000	0.047	1.237	1.285	0.888	
2	0.060	0.000	0.110	0.007	0.178	0.209	
3	0.764	0.000	0.193	0.587	1.545	1.377	1.62
4	3.018	0.005	0.279	0.393	3.694	3.511	3.69
5	2.099	0.068	0.348	0.031	2.546	2.529	2.68
6	0.354	0.436	0.390	0.052	1.232	1.182	1.32
7	1.348	0.970	0.400	0.217	2.934	2.608	2.47
8	0.820	0.282	0.382	0.303	1.786	1.680	1.62
9	0.095	0.280	0.344	0.282	1.000	0.923	1.00
10	0.990	0.189	0.295	0.209	1.683	1.601	1.67
11	0.736	0.330	0.242	0.132	1.440	1.332	1.34
12	0.097	0.003	0.191	0.073	0.363	0.397	

[a]Values from Chiu *et al.* (Ref. 19).

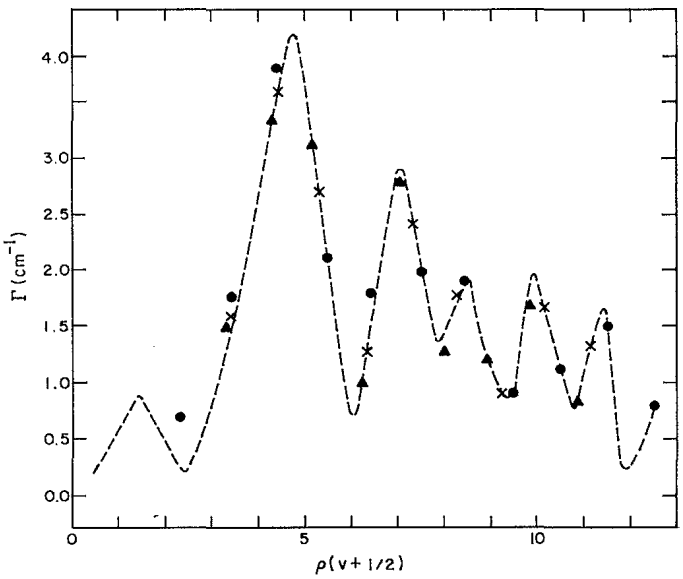

FIG. 2. Variation of predissociation linewidth with vibrational quantum number in the $B\,^3\Sigma_u^-$ state of $^{16}O_2$, $^{16}O^{18}O$, and $^{18}O_2$ as a function of $\rho(v+\frac{1}{2})$. The dashed curve is a curve that passes through the theoretical widths of the three isotopes, calculated as an average of the three F_i components with the same J. The solid circles are the measured widths for $^{16}O_2$ (Ref. 18), the crosses are the measured widths for $^{16}O^{18}O$ (Ref. 19), and the triangles are the measured widths for $^{18}O_2$ (Ref. 19).

TABLE V. The experimental and deperturbed second vibrational energy differences (in cm^{-1}).

	$^{16}O_2$			$^{16}O^{18}O$			$^{18}O_2$		
v	Δ^2S_v	$-\Delta^2G_v$[a]	$-\Delta^2G_v^0$	Δ^2S_v	$-\Delta^2G_v$[b]	$-\Delta^2G_v^0$	Δ^2S_v	$-\Delta^2G_v$[c]	$-\Delta^2G_v^0$
1	−0.404	22.41	22.01	−0.306			−0.201		
2	−0.192	23.90	23.71	−0.310			−0.342		
3	0.529	23.76	24.29	0.374	22.51	22.88	0.238	21.03	21.27
4	1.171	25.98	27.15	1.562	23.88	25.44	1.834	21.83	23.66
5	−2.532	29.79	27.26	−2.613	28.37	25.76	2.417	26.58	24.16
6	2.435	28.42	30.86	2.070	26.42	28.49	1.291	25.28	26.57
7	−1.918	33.04	31.12	−1.582	31.06	29.48	−0.806	27.77	26.96
8	0.570	33.98	34.55	0.686	31.20	31.89	0.530	29.13	29.66
9	0.470	37.62	38.09	0.071	34.75	34.82	−0.454	32.45	32.00
10	−0.788	40.59	39.80	−0.783	37.57	36.79	−0.227	33.92	33.69
11	0.136	42.72	42.86	0.697	39.10	39.80	0.885	36.15	37.04
12	0.468	44.50	44.97	0.188	41.78	41.97	−0.371	38.95	38.58

[a]Obtained from Cheung *et al.* (Ref. 22).
[b]Obtained from Cheung *et al.* (Ref. 17).
[c]Obtained from Cheung *et al.* (Ref. 23).

(9,0) band by using different predissociation widths for the fine structure components of a rotational line is in progress.

C. Level shifts

Besides the broadening of spectral lines the predissociation introduces perturbations into spectroscopic constants, such as rotational constants, fine structure parameters, and band origins.[6,26] As discussed by Julienne and Krauss,[6] it is easier to detect the level shifts introduced by the various interactions than the modifications in the spectroscopic constants. The second vibrational difference

$$\Delta^2G_v=G_{v-1}+G_{v+1}-2G_v \tag{2}$$

is examined, which magnifies the effects. The level shift contribution to the second vibrational energy difference is given by

$$\Delta^2S_v=S_{v+1}+S_{v-1}-2S_v, \tag{3}$$

where S_v is the shift of the vibrational level with quantum number v due to the repulsive states interacting with the $B\,^3\Sigma_u^-$ state. The deperturbed second difference is given by

$$\Delta^2G_v^0=\Delta^2G_v-\Delta^2S_v \tag{4}$$

for the different isotopic molecules.

Table V lists these three second differences. Plots of the second vibrational energy differences $-\Delta^2G_v$ and the deperturbed second differences $\Delta^2G_v^0$ vs vibrational quantum number, v, are presented in Figs. 3, 4, and 5, respectively, for $^{16}O_2$, $^{16}O^{18}O$, and $^{18}O_2$. The smooth deperturbation of the second differences of the three isotopes can be seen in these figures.

In the work of Cheung *et al.*,[17] the calculated level shift contributions to the second vibration energy differences were based on only the $^5\Pi_u$–$B\,^3\Sigma_u^-$ interaction and they concluded that values of the parameters for the $^5\Pi_u$ state of

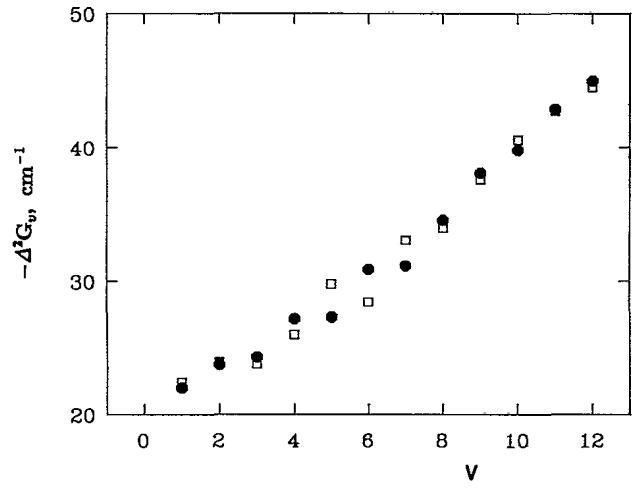

FIG. 3. Plot of second vibrational difference, $-\Delta^2G_v$, vs v for the $B\,^3\Sigma_u^-$ state of $^{16}O_2$. The experimental second differences $-\Delta^2G_v$ are represented by the open squares. The deperturbed second differences $-\Delta^2G_v^0$ are represented by the filled circles.

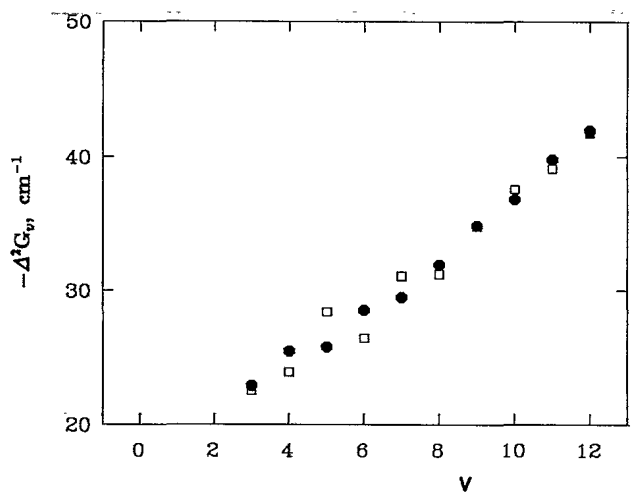

FIG. 4. Plot of second vibrational difference, $-\Delta^2G_v$, vs v for the $B\,^3\Sigma_u^-$ state of $^{16}O^{18}O$. The experimental second differences $-\Delta^2G_v$ are represented by the open squares. The deperturbed second differences $-\Delta^2G_v^0$ are represented by the filled circles.

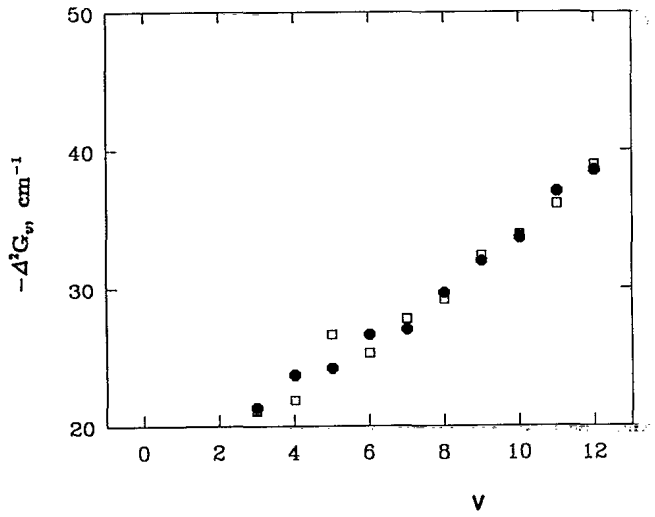

FIG. 5. Plot of second vibrational difference, $-\Delta^2G_v$, vs v for the $B\,^3\Sigma_u^-$ state of $^{18}O_2$. The experimental second differences $-\Delta^2G_v$ are represented by the open squares. The deperturbed second differences $-\Delta^2G_v^0$ are represented by the filled circles.

$A_x = 65\ \text{cm}^{-1}$, $R_x = 1.880$ Å, and $M_x = 40\,000\ \text{cm}^{-1}\ \text{Å}^{-1}$ would best deperturb the observed data. In our present study, contributions from all the four repulsive states are included, which change slightly our earlier values; the new value for A_x is 70 cm^{-1}.

III. DISCUSSION

We have attempted to present a detailed analysis of the predissociation process affecting the Schumann–Runge bands of oxygen. A set of parameters is reported in this work, which gives a smooth deperturbation of the second vibrational energy differences and reproduces all the features in the linewidth pattern of the three isotopic molecules. A comparison of the present and previous parameters is given in Table VI, in which there are three sets of values obtained from the three isotopic molecules by Lewis *et al.*[14,27,28] Since these parameters are isotopically invariant, one set of values should be sufficient to model the predissociation. The results of a recent evaluation of the spin–orbit integrals by Julienne[29] using *ab initio* methods based on multiconfiguration self-consistent field (MCSCF) plus first order configuration interaction (CI) wave function are also listed. Our procedure does not yield the sign of the coupling interaction. The agreement is satisfactory though our results favor a spin–orbit value of $>70\ \text{cm}^{-1}$ in the interaction between the $^5\Pi_u$ state and the $B\,^3\Sigma_u^-$ state, higher than the value of 65 cm^{-1} reported by Julienne.[7,29] Our value is in good agreement with the values published by Lewis *et al.* The two parameters defining the repulsive potential, M_x and R_x are consistent with the earlier results[7,18] and agree with those of Lewis *et al.* except that our uncertainty estimates are smaller in many cases.

The experimental predissociation linewidths of $v = 6,8,9,10,12$ of $^{16}O_2$ reported by Cheung *et al.*[18] and Lewis *et al.*[14] show trends depending on the rotational quantum number, N. With the results of the present study, it is possible to investigate in detail the rotational dependence of predissociation linewidths. We have work in progress to evaluate the linewidths as a function of N for all the three isotopic molecules of oxygen.

ACKNOWLEDGMENTS

We thank Dr. P. S. Julienne for providing unpublished *ab initio* calculation results. A. S-C. C. would like to thank the Smithsonian Institution for the International Exchange Scholarships and the Hung Hing Ying Physical Science Research Fund of the University of Hong Kong for financial support. The work of A. D. and M. J. J. was partly supported by the National Science Foundation, Division of Atmospheric Sciences under Grant No. ATM-9019188. M. F. was a visitor to the Harvard–Smithsonian Institute for Theoretical Atomic and Molecular Physics. This work re-

TABLE VI. Comparison of present and previous model parameters.

State	Parameter	This work	Julienne (1976)[a]	Lewis *et al.* $^{16}O_2$[b]	Lewis *et al.* $^{16}O^{18}O$[c]	Lewis *et al.* $^{18}O_2$[d]	Julienne[e]
$^5\Pi_u$	A_x (cm^{-1})	70±2	65±7	70.9±1.5	69.2±1.8	70.1±2.2	−65
	M_x ($\text{cm}^{-1}\ \text{Å}^{-1}$)	38 600±500	40 000±4 000	39 700±1 000	39 000±1 000	38 700±1 100	
	R_x (Å)	1.879±0.001	1.875±0.002	1.880±0.001	1.880±0.001	1.881±0.001	
$^3\Sigma_u^+$	A_x (cm^{-1})	46±2	55±5	38.8±4.2	40.7±5.0	39.8±3.7	−45
	M_x ($\text{cm}^{-1}\ \text{Å}^{-1}$)	49 000±1 000	45 000±2 500	42 300±8 000	53 000±12 000	34 000±4 000	
	R_x (Å)	1.999±0.001	2.000±0.010	1.996±0.008	1.999±0.005	2.004±0.004	
$^3\Pi_u$	A_x (cm^{-1})	35±3	30	25.8±2.8	28.1±1.8	21.1±3.0	28
	M_x ($\text{cm}^{-1}\ \text{Å}^{-1}$)	74 000±4 000	80 000	62 700±5 000	55 000±2 000	39 000±3 000	
	R_x (Å)	1.429±0.010	1.425	1.441±0.006	1.458±0.003	1.483±0.009	
$^1\Pi_u$	A_x (cm^{-1})	33±5	25±3	32.2±3.0	37.3±6.1	25.2±7.1	25
	M_x ($\text{cm}^{-1}\ \text{Å}^{-1}$)	25 000±3 000	23 000	22 400±1 300	34 000±2 000	21 000±2 000	
	R_x (Å)	1.711±0.010	1.730	1.731±0.003	1.695±0.004	1.735±0.008	

[a]Values from Julienne (Ref. 7).
[b]Values from Lewis *et al.* (Ref. 14).
[c]Values from Lewis *et al.* (Ref. 30).
[d]Values from Lewis *et al.* (Ref. 31).
[e]Results based on MCSCF+first order CI wave function, Julienne (Ref. 32).

ported was also supported by the NASA Upper Atmospheric Research Program under Grant No. NAGS-484 to the Smithsonian Astrophysical Observatory. We are indebted to the referee for the suggestion that led to Fig. 2.

[1] P. Krupenie, J. Phys. Chem. Ref. Data **1**, 423 (1972).
[2] H. F. Schaefer III and W. H. Miller, J. Chem. Phys. **55**, 4107 (1971).
[3] M. Ackerman and F. Biaume, J. Mol. Spectrosc. **35**, 73 (1970).
[4] J. N. Murrell and J. M. Taylor, Mol. Phys. **16**, 609 (1969).
[5] R. D. Hudson and S. H. Mahle, J. Geophys. Res. **35**, 73 (1972).
[6] P. S. Julienne and M. J. Krauss, J. Mol. Spectrosc. **56**, 270 (1975).
[7] P. S. Julienne, J. Mol. Spectrosc. **63**, 60 (1976).
[8] M. L. Sink and A. D. Bandrauk, J. Chem. Phys. **66**, 5313 (1977).
[9] R. Persico, M. Cimiraglia, and J. Tomasi, J. Chem. Phys. **42**, 2970 (1979).
[10] B. R. Lewis, J. H. Carver, T. I. Hobbs, D. G. McCoy, and H. P. F. Gies, J. Quantum Spectrosc. Radiat. Transfer **22**, 213 (1979).
[11] B. R. Lewis, J. H. Carver, T. I. Hobbs, D. G. McCoy, and H. P. F. Gies, J. Quantum Spectrosc. Radiat. Transfer **20**, 191 (1978).
[12] J. E. Frederick and R. D. Hudson, J. Mol. Spectrosc. **74**, 247 (1979).
[13] H. P. F. Gies, S. T. Gibson, D. G. McCoy, A. J. Blake, and B. R. Lewis, J. Quantum Spectrosc. Radiat. Transfer **26**, 469 (1981).
[14] B. R. Lewis, L. Berzins, J. H. Carver, and S. T. Gibson, J. Quantum Spectrosc. Radiat. Transfer **36**, 187 (1986).
[15] M. Nicolet, S. Cieslik, and R. Kennes, Planet. Space Sci. **36**, 1039 (1988).
[16] A. M. Wodtke, L. Hüwel, H. Schüter, H. Voges, G. Meyer, and P. Andresen, J. Chem. Phys. **89**, 1929 (1988).
[17] A. S.-C. Cheung, K. Yoshino, D. E. Freeman, R. S. Friedman, A. Dalgarno, and W. H. Parkinson, J. Mol. Spectrosc. **134**, 362 (1989).
[18] A. S.-C. Cheung, K. Yoshino, J. R. Esmond, S. S.-L. Chiu, D. E. Freeman, and W. H. Parkinson, J. Chem. Phys. **92**, 842 (1990).
[19] S. S.-L. Chiu, A. S.-C. Cheung, K. Yoshino, J. R. Esmond, D. E. Freeman, and W. H. Parkinson, J. Chem. Phys. **93**, 5539 (1990).
[20] D. E. Freeman, A. S.-C. Cheung, K. Yoshino, and W. H. Parkinson, J. Chem. Phys. **91**, 6538 (1989).
[21] X. Yang, A. M. Wodtke, and L. Hüwel, J. Chem. Phys. **94**, 2469 (1991).
[22] A. S.-C. Cheung, K. Yoshino, W. H. Parkinson, and D. E. Freeman, J. Mol. Spectrosc. **119**, 1 (1986).
[23] A. S.-C. Cheung, K. Yoshino, D. E. Freeman, and W. H. Parkinson, J. Mol. Spectrosc. **131**, 96 (1988).
[24] R. P. Saxon and B. Liu, J. Chem. Phys. **67**, 5432 (1977).
[25] M. L. Du, A. Dalgarno, and M. J. Jamieson, J. Chem. Phys. **91**, 2980 (1989).
[26] H. Lefebvre-Brion and R. W. Field, *Perturbations in the Spectra of Diatomic Molecules* (Academic, New York, 1986).
[27] B. R. Lewis, L. Berzins, and J. H. Carver, J. Quantum Spectrosc. Radiat. Transfer **37**, 229 (1987).
[28] B. R. Lewis, L. Berzins, and J. H. Carver, J. Quantum Spectrosc. Radiat. Transfer **37**, 243 (1987).
[29] P. S. Julienne (private communication, 1991).